Posttranslational Modifications of FERREDOXIN-NADP$^+$ OXIDOREDUCTASE in Arabidopsis Chloroplasts[1][W][OPEN]

Nina Lehtimäki[2], Minna M. Koskela[2], Käthe M. Dahlström, Eveliina Pakula, Minna Lintala, Martin Scholz, Michael Hippler, Guy T. Hanke, Anne Rokka, Natalia Battchikova, Tiina A. Salminen, and Paula Mulo*

Molecular Plant Biology, Department of Biochemistry, University of Turku, FI–20520 Turku, Finland (N.L., M.M.K., E.P., M.L., N.B., P.M.); Structural Bioinformatics Laboratory, Department of Biosciences, Åbo Akademi University, FI–20520 Turku, Finland (K.M.D., T.A.S.); Institute of Plant Biology and Biotechnology, Faculty of Biology, Westfälische Wilhelms-Universität Münster, DE–48143 Muenster, Germany (M.S., M.H.); Plant Physiology, Faculty of Biology and Chemistry, University of Osnabrück, DE–49076 Osnabruck, Germany (G.T.H.); and Turku Centre for Biotechnology, FI–20520 Turku, Finland (A.R.)

Rapid responses of chloroplast metabolism and adjustments to photosynthetic machinery are of utmost importance for plants' survival in a fluctuating environment. These changes may be achieved through posttranslational modifications of proteins, which are known to affect the activity, interactions, and localization of proteins. Recent studies have accumulated evidence about the crucial role of a multitude of modifications, including acetylation, methylation, and glycosylation, in the regulation of chloroplast proteins. Both of the Arabidopsis (*Arabidopsis thaliana*) leaf-type FERREDOXIN-NADP$^+$ OXIDOREDUCTASE (FNR) isoforms, the key enzymes linking the light reactions of photosynthesis to carbon assimilation, exist as two distinct forms with different isoelectric points. We show that both AtFNR isoforms contain multiple alternative amino termini and undergo light-responsive addition of an acetyl group to the α-amino group of the amino-terminal amino acid of proteins, which causes the change in isoelectric point. Both isoforms were also found to contain acetylation of a conserved lysine residue near the active site, while no evidence for in vivo phosphorylation or glycosylation was detected. The dynamic, multilayer regulation of AtFNR exemplifies the complex regulatory network systems controlling chloroplast proteins by a range of posttranslational modifications, which continues to emerge as a novel area within photosynthesis research.

Plants adjust their metabolism according to environmental stimuli by inducing adaptation mechanisms, which ultimately lead to changes in intracellular protein levels and activities. In addition to modulating gene expression, which results in relatively long-term changes, rapid responses are required in order to maintain the functionality and fitness of plants upon sudden shifts in ambient conditions. These responses are achieved through posttranslational modifications (PTMs) of proteins (Prabakaran et al., 2012). In general, PTMs of proteins are known to affect enzyme activity, localization, and turnover as well as interaction with other proteins, RNA, DNA, and lipids, thus providing mechanisms for the rapid adjustment of cellular metabolism (Mann and Jensen, 2003). PTMs include proteolytic cleavage and covalent addition of modifying groups to amino acids, such as phosphorylation, acetylation, methylation, and glycosylation.

In chloroplasts, phosphorylation is the best-characterized PTM, which regulates photosynthetic performance and other responses to environmental stimuli. For example, under high light intensity, PSII subunits D1, D2, CHLOROPHYLL BINDING 43-kD PROTEIN (CP43), and PSII REACTION CENTER PROTEIN H are strongly phosphorylated with the simultaneous suppression of light-harvesting complex (LHC) phosphorylation, while a decrease in light intensity results in the opposite phosphorylation pattern (Tikkanen and Aro, 2012). The reversible phosphorylation of PSII and LHCII is a prerequisite for the efficient repair of photodamaged PSII, and it also guarantees balanced excitation of the photosystems, thus preventing oxidative damage of the photosynthetic machinery (Aro et al., 1993; Tikkanen and Aro, 2012).

Recently, acetylation of nonhistone plant proteins has drawn more and more attention (Xing and Poirier, 2012). N$^{\alpha}$-acetylation refers to the addition of an acetyl group to the α-amino group of the N-terminal amino

[1] This work was supported by the Academy of Finland (grant no. 263667), the Finnish Centre of Excellence Molecular Biology of Primary Producers (grant no. 271832 to P.M., N.L., M.M.K., M.L., E.P., and N.B.), the Sigrid Juselius Foundation (to T.A.S. and K.M.D.), the Tor, Joe, and Pentti Borg Foundation (to T.A.S. and K.M.D.), the Åbo Akademi Graduate School (to K.M.D.), the Finnish Doctoral Program in Plant Science (to N.L.), and the Deutsche Forschungsgemeinshaft (grant no. P2 within Sonderforschungsbereich 944 to G.T.H. and grant no. HI739/12-1 to M.H.).

[2] These authors contributed equally to the article.

* Address correspondence to pmulo@utu.fi.

The author responsible for distribution of materials integral to the findings presented in this article in accordance with the policy described in the Instructions for Authors (www.plantphysiol.org) is: Paula Mulo (pmulo@utu.fi).

[W] The online version of this article contains Web-only data.

[OPEN] Articles can be viewed online without a subscription.

www.plantphysiol.org/cgi/doi/10.1104/pp.114.249094

acid of proteins. Cotranslationally occurring N^{α}-acetylation of preprotein transit peptides has been shown to be crucial for efficient translocation into the plastids (Pesaresi et al., 2003; Bischof et al., 2011). In addition to the preproteins, many mature nucleus-encoded chloroplast proteins are targets of posttranslational N^{α}-acetylation inside the chloroplast (Zybailov et al., 2008; Bienvenut et al., 2011, 2012), and a number of chloroplast-encoded proteins, such as D1, D2, CP43, RUBISCO LARGE SUBUNIT, and ATP SYNTHASE ε SUBUNIT (AtpE), have also been shown to be N^{α}-acetylated (Michel et al., 1988; Mulligan et al., 1988; Zybailov et al., 2008; Hoshiyasu et al., 2013). N^{α}-acetylation was shown to protect AtpE from degradation upon drought stress (Hoshiyasu et al., 2013), while no specific role has been defined for the N^{α}-acetylation of the other mature chloroplast proteins. N^{ε}-acetylation of the side chain amino group of Lys residues (Lys acetylation), in turn, is a well-known modification of histone proteins, which regulates the chromatin structure and, thus, affects transcriptional activity (Jenuwein and Allis, 2001). Lys acetylation has only recently been described in nonhistone proteins (Choudhary et al., 2009), including several proteins from the chloroplasts of higher plants (Finkemeier et al., 2011; Wu et al., 2011). Intriguingly, the activity of some central chloroplast proteins, such as Rubisco, phosphoglycerate kinase, and NAD^{+}-dependent malate dehydrogenase, has been shown to change upon Lys acetylation (Finkemeier et al., 2011).

FERREDOXIN-$NADP^{+}$ OXIDOREDUCTASE (FNR) links the light reactions of photosynthesis to stromal metabolism by accepting electrons from two reduced FERREDOXIN (FD) molecules and using them for the reduction of $NADP^{+}$ to NADPH. NADPH, in turn, is mainly used for carbon assimilation. In Arabidopsis (*Arabidopsis thaliana*), chloroplast FNR is encoded by two distinct nuclear genes, *At5g66190* encoding AtFNR1 and *At1g20020* encoding AtFNR2 (Hanke et al., 2005). The mature isoforms share 82% amino acid sequence identity (Fig. 1), and their function is partly redundant. Either AtFNR1 or AtFNR2 alone is able to support the autotrophic growth of plants, although the growth and development of the *fnr1* and *fnr2* single mutant plants are compromised compared with wild-type plants (Lintala et al., 2007, 2009; Hanke et al., 2008). Interruption of both leaf-type *FNR* genes simultaneously results in pale, yellowish plants capable of only heterotrophic growth on Suc medium (Lintala et al., 2012). Based on structural studies, FNR is predicted to be a soluble protein, but it is nonetheless divided into membrane-bound and soluble pools (Hanke et al., 2005). It has been shown that the AtTIC62 (for the 62-kD subunit of the translocon of inner chloroplast envelope; Benz et al., 2009, 2010) and AtTROL (for thylakoid rhodanese-like protein; Jurić et al., 2009) proteins serve as the membrane anchors for AtFNR (Lintala et al., 2014). Despite the partly redundant function and high similarity of the isoforms, AtFNR1 and AtFNR2 show distinct molecular properties,

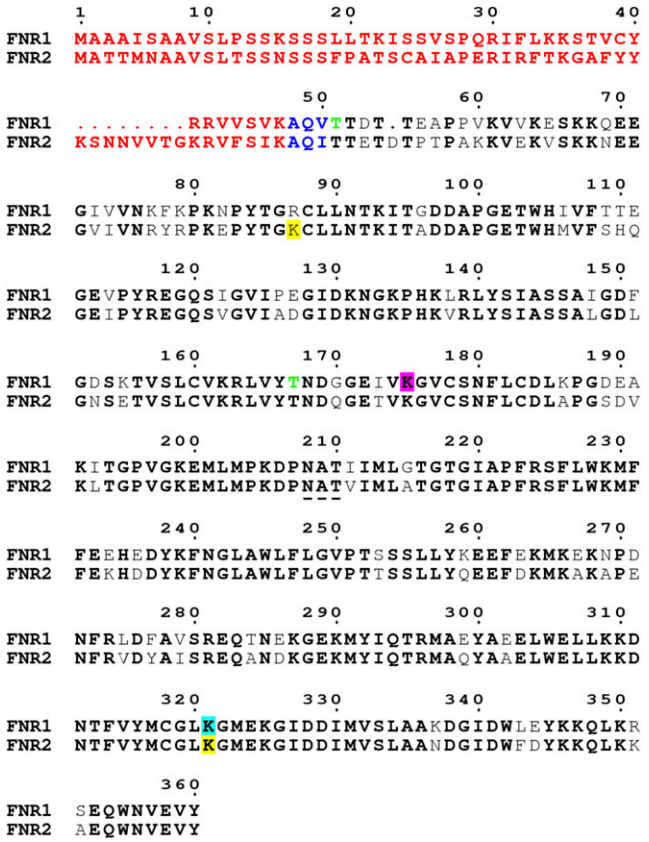

Figure 1. The amino acid sequences of AtFNR1 and AtFNR2 aligned by MALIGN. The transit peptide is denoted in red, and the alternatively trimmed amino acids are denoted in blue. Lys-175 is acetylated in acidic AtFNR1 (pink), Lys-321 in acidic and basic AtFNR1 (turquoise), and Lys-96 and Lys-330 in acidic and basic AtFNR2 (yellow). The underlined NAT denotes the conserved *N*-glycosylation site. The putative phosphorylated Thr residues in the N terminus of FNR1 (Reiland et al., 2009) and Thr-168 in FNR1 (Yang et al., 2013) are shown in green. The numbering is shown for AtFNR1, and conserved residues are in boldface.

as AtFNR1 is required for thylakoid membrane binding of AtFNR2 in planta (Lintala et al., 2007) and upon growth under low temperature only *fnr2* plants show changes in oxidative stress responses. Hence, the AtFNR2 isoform is proposed to have a specific role in directing the reducing power from PSI to stromal reactions (Lintala et al., 2009).

The AtFNR1 and AtFNR2 isoforms can be separated into two forms with different pIs by isoelectric focusing (Lintala et al., 2007), which indicates that both proteins are posttranslationally modified. Therefore, we have now focused on clarifying the type(s) of PTMs of these proteins and their impact on FNR function. In this study, we show that neither of the FNR isoforms is likely to be phosphorylated or glycosylated, whereas Lys acetylation and N-terminal trimming were detected in all four forms of AtFNR. Both AtFNR isoforms were also found to contain partial N^{α}-acetylation, which was attributed to the shift in pI. The generated

three-dimensional (3D) model for the AtFNR1-AtFNR2 heterodimer in complex with the AtTIC62 peptide indicates that the acetylated Lys-321 in AtFNR1 and Lys-330 in FNR2 are located in close proximity to the active site, but none of the detected modifications interfere with AtTIC62 binding. Moreover, the degree of N-terminal acetylation of AtFNR was shown to change in response to light, implying a dynamic control of FNR function through PTMs.

RESULTS

AtFNR1 and AtFNR2 Are N-Terminally Trimmed and N^{α} Acetylated

The AtFNR1 and AtFNR2 isoforms are localized in the chloroplasts, where they are found as soluble proteins as well as bound to the thylakoid and inner chloroplast envelope membranes (Hanke et al., 2005; Lintala et al., 2007; Benz et al., 2009; Fig. 2). After separation of the membrane-bound proteins by isoelectric focusing and two-dimensional (2D) SDS-PAGE, both AtFNR isoforms form two clear spots with different pIs (the acidic [a] and basic [b] forms) but with similar molecular masses (Fig. 2, A and B; Lintala et al., 2007). As the same pattern was identified from the soluble fraction of chloroplast proteins (Fig. 2, C and D), the PTMs do not appear to be the sole determinants of AtFNR localization. Moreover, the additional faint spots in the proximity of AtFNR1 (1 and 2 in Fig. 2A) and AtFNR2 (3 in Fig. 2A) were identified as AtFNR1 and AtFNR2, respectively.

In wheat (*Triticum aestivum*), three amino acid residues in the N terminus of photosynthetic FNRI (pFNRI) and two amino acid residues in pFNRII have been shown to be trimmed, which results in changes in their enzyme activity (Gummadova et al., 2007). Therefore, the N termini of the membrane-bound and soluble pools of AtFNR were analyzed by liquid chromatography-tandem mass spectrometry (LC-MS/MS) after excision of the spots from 2D gels, and several different N-terminal peptides were identified for both AtFNR1 and AtFNR2. The spots representing AtFNR1 (both acidic and basic) contained peptides starting with AQVTTDTT, QVTTDTT, and VTTDTT, and the spots representing AtFNR2 (both acidic and basic) contained N-terminal peptides starting with AQITTETD, QITTETD, and ITTETD (Table I). More peptides starting with Gln and Ile or Val were identified, as compared with those starting with Ala, in both the soluble and membrane-bound FNR pools (Supplemental Table S1). Results from Edman degradation corroborated the LC-MS/MS findings: analysis of the basic AtFNR1 spot revealed two alternative sequences for the N terminus of AtFNR1 (QVTTD and VTTDT) and one for the N terminus of the basic AtFNR2 spot (QITTE; Table II). Sequencing of the acidic spots remained unsuccessful, indicating possible N-terminal blocking of the proteins (Table II), which prompted us to search for possible N-terminal modifications of the proteins. Indeed, several N^{α}-acetylated peptides were detected in the acidic AtFNR1 and AtFNR2 spots in both the membrane-bound and soluble pools, while none (AtFNR1b) or only one (AtFNR2b) was found in the basic spots with high confidence (Table III; Supplemental Table S1). In addition to acetylation, Gln cyclization to pyro-Glu was detected in all FNR forms. Detection of some unmodified peptides in the acidic spots, and of a few modified peptides in the basic spots, might result from incomplete isoelectric focusing during 2D SDS-PAGE. As pyroglutamylated peptides, identified from the Q-starting peptides in all spots, are common artifacts in mass spectrometry (MS) analysis, we conclude that N^{α}-acetylation of FNR is the modification resulting in the appearance and N-terminal blocking of the acidic forms of both AtFNR isoforms in planta.

AtFNR1 and AtFNR2 Are Lys Acetylated

Acetylation and methylation of chloroplast proteins have been identified recently (Houtz et al., 1992; Finkemeier et al., 2011; Wu et al., 2011; Mininno et al., 2012; Alban et al., 2014). Therefore, the acetylation and methylation states of the four membrane-bound AtFNR forms were analyzed. Acetylation of Lys residues results in a mass gain of 42.0105 D due to the substitution of a hydrogen atom with an acetyl group (CH_3CO_2), while trimethylation increases the mass by 42.0471 D. It is important to note that the small 0.03-D mass difference between Lys-acetylated and Lys-trimethylated peptides can be distinguished in the spectra of the LTQ Orbitrap mass spectrometer. All membrane-bound AtFNR forms possessed acetylated Lys residues, while no methylation could be reliably detected (Table IV; Fig. 1). In the acidic AtFNR1 spot, Lys-175 and Lys-321 were found to be acetylated, while in the basic AtFNR1, only Lys-321 acetylation could be detected. Both AtFNR2 spots, in turn, possessed Lys acetylation on Lys-96 and Lys-330 (Table IV; Fig. 1). Lys acetylation could not be assessed reliably from the soluble FNR pool due to the low protein abundance in the soluble fraction.

AtFNR Is Neither Phosphorylated Nor Glycosylated

Both of the AtFNR isoforms contain putative phosphorylation sites (Lintala et al., 2007) and a conserved *N*-glycosylation site (Asn-Ala-Thr; Fig. 1), similar to other leaf-type FNRs (Supplemental Fig. S1). Nevertheless, immunoblot analysis using anti-phospho-Thr, anti-phospho-Ser, or anti-phospho-Tyr antibody, as well as staining the 2D gels with Pro-Q Diamond Phosphoprotein Gel Stain, provided negative results, and no shift in the electrophoretic mobility of AtFNR was detected after phosphatase treatment of immunoprecipitated AtFNR using Phos-tag acrylamide (Supplemental Fig. S2). Moreover, when the isolated membranes were treated either with calf

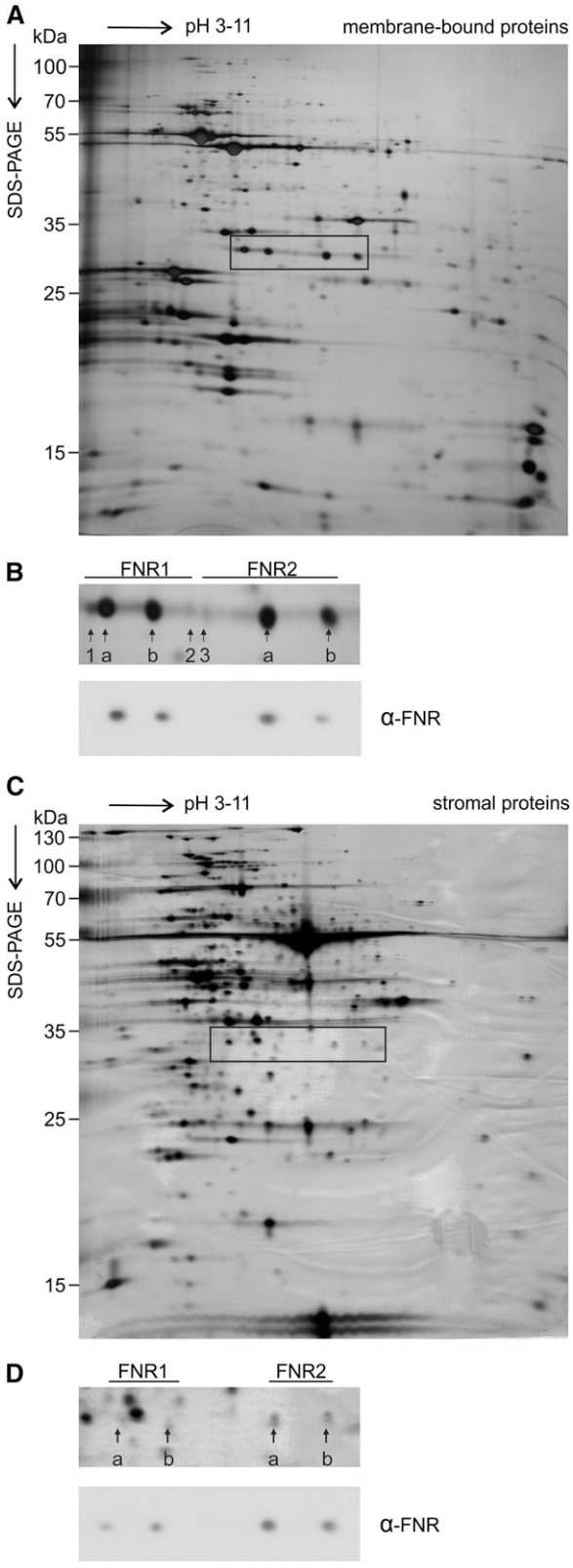

Figure 2. Membrane-bound and stromal proteins of Arabidopsis separated by 2D SDS-PAGE. A, Proteins from the membrane fraction (200 μg) were separated by 2D SDS-PAGE. AtFNR forms are framed. B, AtFNR forms are shown in detail together with a corresponding immunoblot (α-FNR). Protein spots that were analyzed by MS analysis are marked by arrows (a, acidic form; b, basic form; and 1–3, minor forms). C, Proteins of the stroma fraction (200 μg) were separated by 2D SDS-PAGE. The AtFNR forms are framed. D, AtFNR forms are shown in detail together with a corresponding immunoblot (α-FNR).

alkaline phosphatase and Lambda protein phosphatase or with the protein phosphatase inhibitors, the pattern of FNRs on the 2D gels remained unchanged (Supplemental Fig. S2). Staining of the 2D gel with the glycoprotein stain ProQ Emerald Glycoprotein or immunoblotting using a Fuc antibody resulted in a weak signal from all AtFNR spots (Supplemental Fig. S3). As a similar response was also recorded by using a *complex-glycan-deficient* mutant of Arabidopsis, which lacks complex glycans (Strasser et al., 2005), the signal appears to be unspecific. Moreover, LC-MS/MS analysis of putative glycans revealed numerous peptides from the conserved *N*-glycosylation site, but without the expected +3-D mass shift at the Asn (Supplemental Table S2). Although several glycoproteins have been identified in Arabidopsis chloroplasts (Villarejo et al., 2005; Nanjo et al., 2006), our results suggest that AtFNR is not one of those.

Molecular Interactions of FNR

AtFNR is present in several high-molecular-mass (approximately 500 and 190 kD) thylakoid protein complexes together with the AtTIC62 (Benz et al., 2009) and AtTROL (Jurić et al., 2009) proteins, which contain highly similar Pro-rich FNR-binding domains. In principle, each domain is able to bind two FNR molecules. To get insights into the possible role of PTMs in complex formation, the 3D structure of the AtFNR1-AtFNR2 heterodimer in complex with the AtTIC62 peptide (Fig. 3) was modeled. The model is based on the crystallized pea (*Pisum sativum*) FNR (PsFNR)-PsTIC62 complex (Protein Data Bank [PDB] code 3MHP; Alte et al., 2010), where Tyr-308 was rotated into a conformation that allows $NADP^+$ binding. Analysis of the amino acids interacting with PsTIC62 in both chains of the PsFNR dimer and comparison with those of AtFNR1 and AtFNR2 show that the residues in AtFNR1 have a similar conservation rate with both the A and B chains, while AtFNR2 residues are more conserved with the A chain. Hence, to create the 3D model of the heterodimeric AtFNR1-AtFNR2 complex with AtTIC62, we modeled AtFNR2 in the position of the A chain and AtFNR1 in the position of the B chain of the PsFNR homodimer. The model evaluations show that the 3D fold can be considered reliable and that the model is of good quality, with 93.6% of the residues in most favored regions in the Ramachandran plot produced by PROCHECK (Laskowski et al., 1993). The high sequence identity between the PsFNR and AtFNRs further increases the reliability of the 3D models.

Table I. *N-terminal sequences of the acidic and basic AtFNR1 and AtFNR2 proteins determined by MS analysis*

The membrane proteins of Arabidopsis plants were separated by 2D gel electrophoresis. The four spots representing AtFNR1 and AtFNR2 were excised from the gel, digested with trypsin, and subjected to LC-MS/MS using the LTQ Orbitrap Velos Pro mass spectrometer.

Isoform	Peptide Sequence	Mass Measured	Change	Expectation Value	Ion Score
			ppm		
FNR1	AQVTTDTTEAPPVK	1,457.749	0.21	1.60E-05	78
	QVTTDTTEAPPVK	1,386.711	0.14	1.80E-04	67
	VTTDTTEAPPVK	1,258.652	−0.25	2.40E-04	66
FNR2	AQITTETDTPTPAK	1,473.7387	−3.05	3.30E-04	66
	QITTETDTPTPAK	1,402.70586	−0.15	5.90E-05	73
	ITTETDTPTPAK	1,274.646	−1.14	2.80E-06	86

In the modeled complex, the AtTIC62 peptide holds the AtFNR1-AtFNR2 heterodimer together in a back-to-back conformation (Fig. 3), which is further stabilized by interactions between Arg-87, Leu-89, Leu-90, Thr-109, and Pro-187 in AtFNR1 and Leu-98, Leu-99, Leu-160, Asn-162, Glu-164, Pro-196, and Gly-197 in AtFNR2. Importantly, none of the acetylated Lys residues coincide with the binding sites of AtTIC62; thus, the Lys acetylations are not likely to regulate the membrane binding of FNR, at least directly. This result is in line with the fact that all four FNR spots are present in both the membrane-bound and soluble pools (Fig. 2). Moreover, we separated the thylakoid protein complexes by blue native (BN)-PAGE and analyzed the FNR-containing protein complexes using LC-MS/MS (Fig. 4). Even if the complex of approximately 500 kD is known to be composed of FNR and TIC62 (Benz et al., 2009) and the complex of 190 kD is known to be composed of FNR and TROL (Jurić et al., 2009), all the studied complexes contained both AtFNR isoforms as well as TIC62 and TROL, which indicates an incomplete separation capacity of BN-PAGE (Fig. 4). All complexes also contained alternatively trimmed N termini of AtFNR, but the other types of PTMs were not reliably detected, possibly due to the high number of other proteins present in the complexes. As the long and flexible N terminus of FNR does not allow reliable structural modeling (Fig. 3), the question about the effect of N-terminal trimming on the interaction of AtFNR with either TIC62 or TROL still remains open.

Next, we wanted to clarify whether the PTMs could have an effect on the interaction of FNR with FD. AtFD1 and AtFD2, representing approximately 5% to 10% and 90% of the total chloroplast FD pool, respectively (Hanke et al., 2004), share 87.2% sequence identity with each other. Interaction of FD with FNR, studied in numerous species, depends on the charges, hydrophobic forces, and conformational changes of both proteins (Jelesarov and Bosshard, 1994; Martínez-Júlvez et al., 2009; Lee et al., 2011; Hanke and Mulo, 2013), and both AtFD isoforms are known to interact with AtFNR in a very similar way (Hanke et al., 2004). There are two available crystal structures of FNR in complex with FD: maize (*Zea mays*) FNR (ZmFNR; PDB code 1GAQ; Kurisu et al., 2001) and *Anabaena* sp. PCC7119 FNR (PDB code 1EWY; Morales et al., 2000). As the sequence identity of AtFNR1 (86.5%) and AtFNR2 (84.1%) to ZmFNR is higher than those for *Anabaena* sp. PCC7119 FNR (51.5% and 51.8%, respectively), only the ZmFNR-ZmFD complex was used for studying the AtFNR-AtFD interaction. Comparison of the FD-binding amino acids in ZmFNR with those in PsFNR, AtFNR1, and AtFNR2 shows that these amino acids or their chemical properties are strictly conserved (Supplemental Fig. S4). Additionally, the amino acids on ZmFD interacting with ZmFNR (Kurisu et al., 2001) are conserved in both AtFD isoforms (Supplemental Fig. S5), indicating that both AtFNR isoforms interact with both AtFDs through identical salt bridges. Of the conserved residues,

Table II. *N-terminal sequences of the acidic and basic membrane-bound AtFNR1 and AtFNR2 proteins determined by Edman degradation*

The membrane proteins of Arabidopsis plants were separated by 2D gel electrophoresis and electroblotted, and the membrane was stained with Coomassie Brilliant Blue. The FNR spots were excised, and N-terminal sequencing was performed using the Procise 494A sequencer. The previously identified N-terminal sequences are also indicated. a denotes acidic form, and b denotes basic form. –, Sequence not detected.

Protein	N-Terminal Sequences	Reference
FNR1	VTTDTT	Hanke et al. (2005)
FNR1a	–	This study
FNR1b	QVTTDT	This study
	VTTDTT	This study
FNR2	ITTETD	Hanke et al. (2005)
FNR2a	–	This study
FNR2b	QITTETD	This study

Table III. *Summary of the N-terminal modifications in the acidic and basic membrane-bound AtFNR1 and AtFNR2 proteins*

The membrane proteins of Arabidopsis plants were separated by 2D gel electrophoresis. The four spots representing AtFNR1 and AtFNR2 were excised from the gel, digested with trypsin, and subjected to LC-MS/MS using the LTQ Orbitrap Velos Pro mass spectrometer. a denotes acidic form, and b denotes basic form.

Isoform	Peptide Sequence	Modification	Mass Measured	Change	Ion Score	Expectation Value
				ppm		
FNR1a	QVTTDTTEAPPVK	N terminus (Gln → pyro-Glu)	1,369.6845	−0.09	67	1.60E-04
	QVTTDTTEAPPVK	N terminus (acetyl)	1,428.7203	−1.02	62	5.50E-04
	VTTDTTEAPPVK	N terminus (acetyl)	1,300.6630	−0.29	52	6.00E-03
FNR1b	QVTTDTTEAPPVK	N terminus (Gln → pyro-Glu)	1,369.6850	0	55	2.40E-03
FNR2a	AQITTETDTPTPAK	N terminus (acetyl)	1,515.7551	0.86	60	9.70E-04
	QITTETDTPTPAK	N terminus (Gln → pyro-Glu)	1,385.6802	0.51	61	5.90E-04
	QITTETDTPTPAK	N terminus (acetyl)	1,444.7177	0.74	81	8.30E-06
	ITTETDTPTPAK	N terminus (acetyl)	1,316.6583	0.15	78	1.60E-05
FNR2b	QITTETDTPTPAK	N terminus (Gln → pyro-Glu)	1,385.6789	−0.46	70	8.30E-05
	QITTETDTPTPAK	N terminus (acetyl)	1,444.7170	0.23	65	3.70E-04

Glu-312 in spinach (*Spinacia oleracea*) FNR is essential for electron transfer between FNR and FD (Aliverti et al., 1998), which is also reflected by its strict conservation in ZmFNR, PsFNR, AtFNR1, and AtFNR2. Furthermore, Phe-65 in *Anabaena* sp. PCC7119 FD has been proposed to be important for the rapid electron transfer to FNR (Hurley et al., 1993). However, the corresponding residue, Tyr-63 in ZmFD, does not seem to be important for the electron transfer (Kurisu et al., 2001), although the aromatic property of the residue is conserved in the aligned proteins (Supplemental Fig. S5). Importantly, even if Lys-321 in AtFNR1 and Lys-330 in AtFNR2 are located in close proximity to the active site, Lys acetylation does not appear to sterically hinder the binding of either AtFD isoform.

Although structural modeling could not resolve the impact of N termini on the molecular interactions (see above), we studied the effect of N^{α}-acetylation on FD binding experimentally. To this aim, mature AtFD1 and AtFD2 were expressed in *Escherichia coli*, purified, and covalently bound to a Sepharose resin. Thereafter, crude protein extract from Arabidopsis leaves was loaded on the FD columns, and the proteins bound to AtFD1 or AtFD2 were analyzed by 2D SDS-PAGE. Figure 5 shows that although both AtFD isoforms are able to bind all four forms of AtFNR, more acidic (N^{α}-acetylated) AtFNR forms as compared with basic (nonacetylated) AtFNRs were bound by both AtFDs in vitro.

Although one of the acetylated Lys residues, Lys-321 (AtFNR1)/Lys-330 (AtFNR2), is situated close to the NADP(H)-binding site (Fig. 3), 3D modeling did not provide proof that the acetylation would limit the access of FAD or $NADP^+$ to the cofactor-binding sites. However, this Lys is conserved (Supplemental Fig. S4) and occupies the same position in the 3D model (Fig. 3) when AtFNR1 and AtFNR2 are compared, which may indicate a role of Lys-321/Lys-330 acetylation in the regulation of enzyme activity or other molecular interactions. The other acetylation sites, Lys-175 in AtFNR1 and Lys-96 in AtFNR2, are located very differently: Lys-175 in AtFNR1 points toward the solvent, while Lys-96 in AtFNR2 is at the interface between the two monomers in the heterodimeric complex (Fig. 3).

The N^{α}-Acetylation Status of FNR Is Regulated by Light

Protein import (Hirohashi et al., 2001) and the accumulation of AtFNR-containing protein complexes at the thylakoids (Benz et al., 2009) depend on the chloroplast redox state, which is strictly regulated by light. We investigated the distribution of the different

Table IV. *Summary of Lys-acetylated peptides of acidic and basic membrane-bound AtFNR1 and AtFNR2 proteins*

The membrane-bound proteins of Arabidopsis plants were separated by 2D gel electrophoresis. The four spots representing AtFNR1 and AtFNR2 were excised from the gel, digested with trypsin, and subjected to LC-MS/MS using the LTQ Orbitrap Velos Pro mass spectrometer. a denotes acidic, form and b denotes basic form.

Arabidopsis Genome Initiative Code	Protein	Peptide	Side Chain Site and Type (A, Acetylation Site)	Mass Measured	Change	Expectation Value	Ion Score
					ppm		
At5g66190	FNR1a	LVYTNDGGEIVKGVCSNFLCDLKPGDEAK	K175A	3,254.57077	−0.05	3.8E-005	52
		DNTFVYMCGLKGMEK	K321A	1,834.81792	0.32	2.0E-004	42
At5g66190	FNR1b	DNTFVYMCGLKGMEK	K321A	1,834.81804	0.39	1.1E-004	45
At1g20020	FNR2a	EPYTGKCLLNTK	K96A	1,465.73467	−0.63	9.8E-004	40
		DNTFVYMCGLKGMEK	K330A	1,834.81816	0.45	3.0E-003	30
At1g20020	FNR2b	EPYTGKCLLNTK	K96A	1,465.73552	−0.05	2.4E-003	36
		DNTFVYMCGLKGMEK	K330A	1,834.81792	0.32	9.4E-003	25

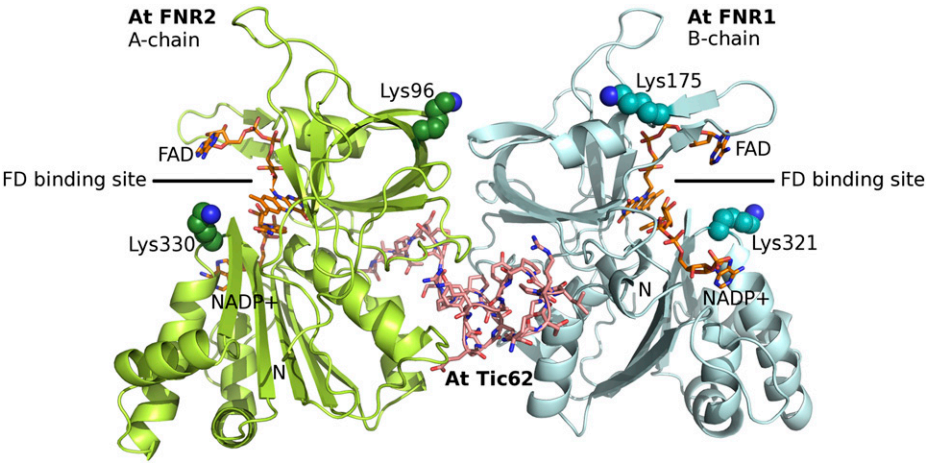

Figure 3. 3D structural model of the AtTIC62-mediated AtFNR1-AtFNR2 heterodimer. AtFNR1 (cyan) and AtFNR2 (green) form a back-to-back complex with AtTIC62 (pink sticks) bound between the subunits. Of the acetylated Lys residues (spheres in teal [AtFNR1] and dark green [AtFNR2]), Lys-321/Lys-330 (AtFNR1/AtFNR2) are located at the same 3D positions in the respective subunits close to the binding sites of the cofactors [orange sticks; NADP(H)] and FAD. Lys-96 (AtFNR2) is close to the dimer interface, while Lys-175 (AtFNR1) is on the surface of the protein.

AtFNR forms in the membrane-bound and soluble pools upon various light conditions in order to see whether some form(s) dominate during the photosynthetically inactive period of the day and whether some of those are needed upon the activation of light reactions or when the photosynthetic machinery is challenged with high irradiation. To this end, leaf samples were collected at the end of the dark period, at growth light (100 μmol photons m^{-2} s^{-1}), and after a 2-h moderate high light treatment (550 μmol photons m^{-2} s^{-1}). Thereafter, the membrane-bound and soluble proteins were isolated, separated by 2D SDS-PAGE, and detected by immunolabeling with FNR antibody. Blots were quantified, and the relative amounts of different forms were determined by comparing the intensity of the spots with the total AtFNR amount on the blot (Fig. 6). Distribution of the soluble AtFNR forms in the dark differed drastically from those in the light. In darkness, AtFNR1 was clearly more abundant than AtFNR2, but upon the shift to light, the relative amount of soluble AtFNR2 increased drastically (Fig. 6, A and B). In contrast, no such significant differences were observed in the distribution of the thylakoid-bound AtFNR forms between the different treatments (Fig. 6, C and D). In addition, the proportion of non-N^{α}-acetylated AtFNR1 (FNR1b) increased with increasing illumination both at membranes and in the soluble fraction compared with the nonacetylated form. A similar trend, but less pronounced, was also observed for the AtFNR2 acidic and basic forms.

DISCUSSION

Recent studies have shown that the processing of organelle-targeting peptides is not as precise as earlier considered, and many chloroplast-imported proteins may contain up to five different transit peptide cleavage positions in their sequence, distributed along a string of 10 amino acid residues (Bienvenut et al., 2012). It is noteworthy that the proteins with multiple cleavage sites contain significantly more frequently Ala at positions −1, 2, 3, 4, and 5 than the proteins with only a single cleavage site (Bienvenut et al., 2012), which also holds true for both AtFNR1 and AtFNR2 (Fig. 1). Nevertheless, it is not yet known whether the Ala residues as such are required for differential cleavage or whether the absence of hydroxylated or acidic amino acid residues interferes with the cleavage of the transit peptide (Bienvenut et al., 2012). In spite of the fact that many chloroplast proteins undergo N-terminal trimming (Zybailov et al., 2008; Plöscher et al., 2009; Bienvenut et al., 2012), this concept seems to be overlooked, perhaps because of its unknown physiological relevance. Some examples are Cys synthase, whose N terminus may start with either the sequence AVSIKPEA or VSIKPEA (Zybailov et al., 2008), and NADPH-protochlorophyllide oxidoreductase A, starting with either AAAVSAP or AAVSAP (Plöscher et al., 2009). To date, there are no data available allowing conclusions about whether the alternative

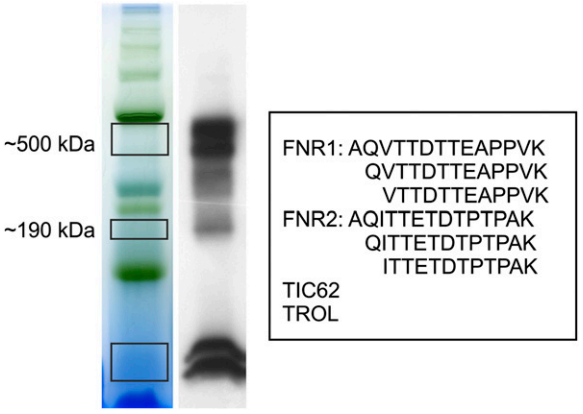

Figure 4. N termini of AtFNR1 and AtFNR2 in the FNR-containing thylakoid protein complexes. Arabidopsis thylakoid protein complexes were separated using BN-PAGE (left). One of the strips was immunolabeled with an FNR antibody (right), and corresponding bands were cut from the gel, digested with trypsin, and subjected to LC-MS/MS using the LTQ Orbitrap Velos Pro mass spectrometer. The identified N termini are shown in the box at right. Also, AtTIC62 and AtTROL were found in all complexes.

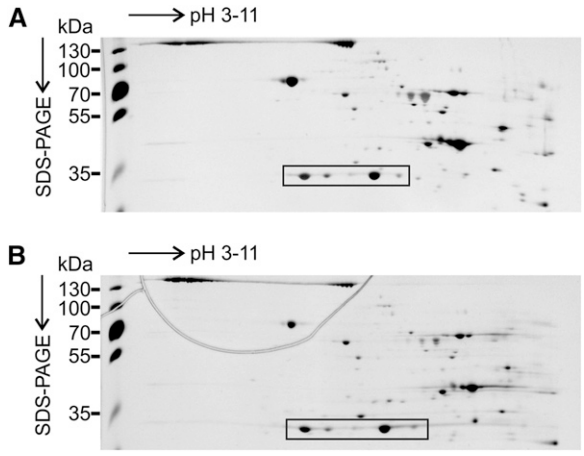

Figure 5. Analysis of interaction partners of chloroplast AtFD isoforms. Arabidopsis proteins bound to recombinant AtFD1 (A) and recombinant AtFD2 (B). Crude leaf extract was incubated with the given AtFD isoform covalently bound to a Sephadex G-25 column. The eluted proteins were separated by 2D SDS-PAGE. AtFNRs are indicated with boxes.

trimming might result from a nonprecise transit peptide cleavage by stromal processing peptidase or from the action of chloroplast aminopeptidases (Zybailov et al., 2008). In fact, several aminopeptidases are known to be located in chloroplasts, and after the cleavage of the transit peptide, they may cleave N-terminal residue(s) and reveal penultimate amino acids (Walling, 2006). This, in turn, may directly affect the longevity of the proteins, thus influencing metabolic reactions (Walling, 2006).

Our results show alternative N-terminal trimming of AtFNR isoforms in both the membrane-bound and soluble AtFNR pools (Tables I and II; Supplemental Table S1) as well as in all AtFNR-TIC62/TROL protein complexes at the thylakoid membrane (Fig. 4). This indicates that the trimming of the AtFNR N terminus would not determine recruitment of the protein into different protein complexes at the thylakoid membrane. Dimerization and membrane association of the three ZmFNR isoforms have been shown to depend on structural variation in the N termini (Twachtmann et al., 2012), but the impact of N-terminal trimming has not yet been studied. Two alternative N termini have also been reported for the wheat pFNRI and pFNRII isoforms: KKVSKKQE and SKKQE for pFNRI and ISKKQD and KKQD for pFNRII (Gummadova et al., 2007). The longer form of pFNRII was able to discriminate between the ZmFD isoforms, but the truncation of two amino acid residues eliminated this ability (Gummadova et al., 2007; Bowsher et al., 2011). It should be noted that the N-terminal start point of the mature wheat pFNRI and pFNRII is 19 to 23 amino acids after the end of the predicted transit peptide, while the N termini of AtFNR1 and AtFNR2 match with the predicted cleavage site (Moolna and Bowsher, 2010), which may indicate differences in the functional properties of the FNR N termini between the species. Nevertheless, as the flexible N terminus of AtFNR does not allow structural modeling (Fig. 3), the ultimate role of N-terminal trimming of AtFNR requires further biochemical analyses.

N^{α}-acetylation of proteins is a major PTM taking place in eukaryotes (Ferro et al., 2003; Meinnel et al., 2005; Kleffmann et al., 2007; Bienvenut et al., 2012). Although it is not a common phenomenon among prokaryotes, it has been described in both nucleus- and chloroplast-encoded plastid proteins (Bienvenut et al., 2011, 2012). In Arabidopsis, about 30% of the N^{α}-acetylation is related to chloroplast proteins translocated via the translocon of outer/inner chloroplast envelope system (Bienvenut et al., 2012), and our results also show that AtFNR belongs to this group (Table III). It has been shown that N^{α}-acetylation occurs preferentially at Ala, Val, and Ser in Arabidopsis (Zybailov et al., 2008) or Ala, Val, Ile, Ser, and Thr in *Chlamydomonas reinhardtii* (Bienvenut et al., 2011). Indeed, the N-terminal peptides representing the N^{α}-acetylated AtFNR1 (FNR1a) started with Val or Gln and the N-terminal peptides representing the N^{α}-acetylated AtFNR2 (FNR2a) started with Ala, Ile, or Gln (Table III; Supplemental Table S1). However, similar N-terminal peptides were also identified in non-acetylated forms, mainly in the basic spots (FNR1/2b), indicating that AtFNRs undergo partial N^{α}-acetylation independent of the N-terminal trimming. In a recent study, it was shown that partial N-terminal acetylation of the ε-subunit of ATP synthase in *Citrullus lanatus* resulted in a practically identical migration pattern on the 2D gels as compared with that of AtFNR (Hoshiyasu et al., 2013). In this case, N^{α}-acetylation was shown to protect the protein from degradation under drought stress conditions (Hoshiyasu et al., 2013).

It has been suggested that the phosphorylation of FNR might provide another level of regulation by determining whether cyclic or linear electron transfer flow is supplied with electrons (Hodges et al., 1990). Indeed, in vitro phosphorylation of pea FNR has been detected (Hodges et al., 1990), and a large-scale Arabidopsis chloroplast phosphoproteome profiling study reported a phosphopeptide, $_{164}$LVY*p***T**NDGGEIVK, for AtFNR1 (Fig. 1; Yang et al., 2013). Additionally, the four distinct wheat FNR spots observed after 2D SDS-PAGE matched the theoretical pIs predicted for phosphorylated FNRs (Moolna and Bowsher, 2010). In contrast, Sugiyama et al. (2008) did not report AtFNR as a phosphoprotein. In this study, we performed a number of experiments trying to gain evidence for AtFNR phosphorylation (Supplemental Fig. S2). Although our results do not completely exclude the possibility that AtFNR isoforms could be phosphorylated, at least under some environmental conditions, we could not find any evidence that AtFNRs would be phosphorylated in planta.

Lys acetylation of several membrane-bound and soluble proteins, such as the ATP/ADP translocator

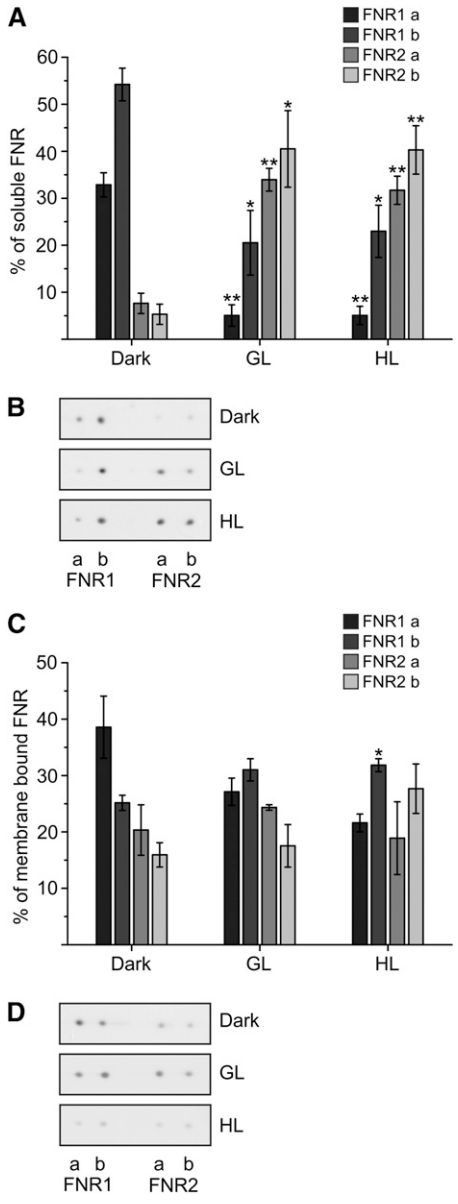

Figure 6. Relative amounts of acidic and basic AtFNR forms in different light conditions. Soluble and membrane-bound proteins were separated by 2D SDS-PAGE and immunoblotted with anti-FNR antibody. Spots were quantified from three to four biological replicates, and the relative amounts from the total FNR pool were calculated. A, Relative amounts of different FNR forms in the soluble fraction of Arabidopsis leaf proteins. B, Representative western blots from the soluble protein fraction from each light condition. C, Relative amounts of different AtFNR forms in the membrane-bound fraction of Arabidopsis leaf proteins. D, Representative western blots from the membrane-bound fraction from each light condition. Dark, Samples collected at the end of the dark period of the day; GL, samples collected from growth light (100 μmol photons m^{-2} s^{-1})-adapted plants in the middle of the light period of the day; HL, samples collected after 2 h of moderate high-light treatment (500–600 μmol photons m^{-2} s^{-1}). Error bars indicate SE; $n = 3$ to 4. AtFNR amounts in growth light and high light were compared with dark amounts using a two-tailed independent Student's t test: $^{*}P < 0.05$ and $^{**}P < 0.01$.

AAC1, ATP synthase, Rubisco, and various LHC proteins, was recently detected in the chloroplast proteome (Finkemeier et al., 2011; Wu et al., 2011). Acetylation of Lys may affect enzyme activity and/or protein-protein interactions by hindering the formation of hydrogen bonds, depending on the position of the Lys residue within the protein. Indeed, the activities of Rubisco and phosphoglycerate kinase increased upon in vitro deacetylation by HUMAN SIRTUIN-3, a broad substrate specificity Lys deacetylase, whereas the activity of malate dehydrogenase decreased (Finkemeier et al., 2011). Intriguingly, it has been shown that the peripheral pool of LHCB1 and LHCB2 possesses a high level of Lys acetylation, whereas the LHC proteins present in the PSII supercomplexes are less acetylated (Wu et al., 2011). Although acetylation of Lys was not found to be light responsive (Wu et al., 2011), these results indicate a regulatory impact of Lys acetylation on photosynthetic reactions and yield. Nevertheless, the location of the acetylated Lys residues on the surface of AtFNR1 and AtFNR2 suggests that these modifications do not affect the interaction with the AtTIC62 and AtTROL proteins (Fig. 3). However, as AtFNR1 (Lys-321) and AtFNR2 (Lys-330) acetylation occurs on a conserved Lys residue in the same 3D position near the active site (Fig. 3; Supplemental Fig. S4), it is plausible that acetylation of Lys-321/330 affects the enzyme activity, even if the 3D models could not provide direct evidence for restricted binding of AtFD, FAD, or $NADP^{+}$ to the acetylated AtFNR isoforms. Interestingly, a conserved Lys-175 in AtFNR1 was acetylated while the corresponding residue in AtFNR2 was not (Table IV), which could confer distinguishing features between the isoforms. It is also tempting to speculate that the acetylation of surface Lys residues in AtFNR might mediate weaker interactions with other (photosynthetic) protein complexes.

A shift from darkness to light affected the ratio of N^{α}-acetylated to nonacetylated forms of AtFNR (Fig. 6), suggesting that N^{α}-acetylation plays a role in the adaptation of the plants to ambient environmental conditions. The relative ratio of all membrane-bound AtFNR forms remained quite stable in all light conditions studied, while the soluble pool showed marked fluctuations (Fig. 6). Upon the transition from darkness to light, the relative amount of both AtFNR2 forms increased drastically compared with AtFNR1. This result suggests a central role for AtFNR2 in light-dependent metabolism, which is in line with our previous results showing a decreased rate of carbon assimilation in the *fnr2* mutant plants as compared with the wild type and *fnr1* (Lintala et al., 2009).

Taken together, our results show that AtFNR is under a complex, multilayer regulation dynamically responding to ambient environmental conditions. In addition to regulation at the levels of gene expression (Hanke et al., 2005; Gummadova et al., 2007), protein import (Hirohashi et al., 2001), and subchloroplastic location (Benz et al., 2009), AtFNR is subjected to N-terminal trimming, N^{α}-acetylation, and acetylation

of Lys residues. The development of novel techniques enabling the identification of various PTMs is likely to reveal other chloroplast proteins that may be regulated by a number of PTMs. The functional significance of these modifications on chloroplast proteins in general, and specifically on AtFNR, obviously requires further research.

MATERIALS AND METHODS

Plant Material and Growth Conditions

Arabidopsis (*Arabidopsis thaliana*) ecotype Columbia plants were grown in a phytotron under standard conditions (100 μmol photons m^{-2} s^{-1}, 8-h-light/16-h-dark cycle, and +23°C). Four- to 5-week-old plants were used in all experiments unless mentioned otherwise. High-light treatment was performed under 500 to 600 μmol photons m^{-2} s^{-1} for 2 h. Temperature measured under the high-light conditions was +28°C to 30°C. Dark samples were taken at the end of the 16-h-dark period prior to the light period.

Isolation of Chloroplasts

Isolation of chloroplasts was performed as described (Zhang et al., 1999) with slight modifications. Leaves of 6-week-old plants were harvested and briefly homogenized in buffer (50 mM HEPES-KOH, pH 7.6, 330 mM sorbitol, 5 mM EDTA, 1 mM $MgCl_2$, 2.5 mM ascorbate, and 0.025% [w/v] bovine serum albumin), filtered through Miracloth (Calbiochem, Merck), and centrifuged (950*g*, 1.5 min, and 4°C). Buffer A (50 mM HEPES-KOH, pH 8, 330 mM sorbitol, and 2 mM EDTA) was used to resuspend the chloroplast-containing pellets before loading them on top of Percoll (Amersham Pharmacia Biotech) step gradients (40% [v/v] and 70% [v/v] in buffer A). After centrifugation (4,000*g*, 5 min, and 4°C), intact chloroplasts were collected from the border of the gradients, washed two times gently with buffer A (centrifuged at 1,250*g*, 1.5 min, and 4°C and at 800*g*, 1 min, and 4°C), and finally resuspended in buffer A.

Isolation of Proteins

For the extraction of leaf proteins, leaf material was frozen in liquid nitrogen. For the isolation of membrane proteins with intact protein complexes, leaves were homogenized in grinding buffer (330 mM sorbitol, 50 mM HEPES-NaOH, pH 7.5, 2 mM EDTA, and 1 mM $MgCl_2$), filtered through Miracloth (Calbiochem, Merck), and centrifuged (4,000*g*, 5 min, and 4°C). The pellet was resuspended in shock buffer (10 mM HEPES-KOH, pH 7.6, 5 mM Suc, and 5 mM $MgCl_2$) and centrifuged (4,000*g*, 5 min, and 4°C), and the resulting pellet was resuspended in storage buffer (10 mM HEPES-KOH, pH 7.5, 100 mM Suc, 5 mM NaCl, and 10 mM $MgCl_2$).

For total protein extraction and fractionation into soluble and membrane fractions, leaves were homogenized directly in shock buffer and filtered through Miracloth. Total protein samples were collected, and the rest of the homogenate was centrifuged (18,600*g*, 5 min, and 4°C). Supernatant was stored as the soluble fraction, and the pellet was resuspended into storage buffer to obtain the membrane fraction. Isolation was performed in the presence of Complete Protease Inhibitor Cocktail Tablets in the shock buffer (Roche Diagnostics).

To further separate membrane and stroma fractions from isolated chloroplasts, intact chloroplasts were centrifuged (9,500*g*, 2 min, and 4°C), and the pellets were resuspended in shock buffer, incubated 10 min on ice, frozen with liquid nitrogen, melted, and centrifuged (18,600*g*, 10 min, and 4°C). Supernatants were stored as stroma fractions, and pellets that were resuspended in storage buffer were stored as membrane fractions.

Immunoprecipitation of AtFNR

Immunoprecipitation of AtFNR was performed by lysing chloroplasts (4 μg of chlorophyll) isolated either in the absence or presence of 10 mM NaF in 100 μL of immunoprecipitation buffer (50 mM Tris-HCl, pH 7.5, and 150 mM NaCl) with 1.5% (w/v) decylmaltoside either in the presence or absence of 10 mM NaF. Chloroplast lysate was centrifuged at 9,500*g* for 10 min at 4°C. The resulting supernatant was incubated with 0.4 μL of FNR antibody and 40 μL of Protein A (Miltenyi Biotec) for 50 min on ice. The mixture was loaded into rehydrated μMACS columns (Miltenyi Biotec), and the columns were washed four times in 200 μL of immunoprecipitation buffer containing 0.15% (w/v) decylmaltoside and one time in 100 μL of 1× Thermo Scientific buffer.

Phosphatase Treatments

The immunoprecipitated AtFNR proteins were subjected to phosphatase treatment (immunoprecipitated AtFNR equal to 4 μg of chlorophyll and 20 μL of calf intestinal alkaline phosphatase (CIP) in Thermo Scientific buffer). Reaction was carried out at +30°C for 30 min. Columns were rinsed with 100 μL of 1× NEB Lambda protein phosphatase buffer (New England Biolabs) and subjected to Lambda phosphatase (New England Biolabs) treatment (10 μL of Lambda phosphatase, NEB protein metallophosphatase buffer, and +37°C for 30 min). Control reactions contained only corresponding buffers.

In vitro protein phosphatase treatment of membrane proteins was performed using Lambda protein phosphatase (New England Biolabs) and CIP alkaline phosphatase (New England Biolabs). Membrane extract (25 μg of chlorophyll) was first treated with CIP alkaline phosphatase (500 units) for 30 min at +37°C and centrifuged (4,000*g*, 5 min, and +4°C). The pellet was resuspended in 1× NEB Lambda protein phosphatase buffer in the presence of Lambda protein phosphatase (16,000 units) and incubated for 30 min at +30°C. Alternatively, the membrane proteins were isolated in the presence of phosphatase inhibitors (PhosSTOP; Roche Diagnostics) and 10 mM NaF. The treated proteins were separated by 2D SDS-PAGE and stained with either silver stain or Pro-Q Diamond Phosphoprotein Gel Stain.

Detection of Glycosylation

Proteins were isolated and separated by 2D SDS-PAGE using standard methods. The gels were either stained with Pro-Q Emerald Glycoprotein Gel Stain (Molecular Probes) or electroblotted and the membrane immunolabeled with a Fuc antibody purchased from Agrisera.

For MS analysis, protein spots were excised from Coomassie Brilliant Blue-stained 2D gels and subsequently destained, reduced, and alkylated as described (Shevchenko et al., 2006). After complete dehydration by two washes with MS-grade acetonitrile, gel pieces were incubated with 500 units (1 μL) of peptide-*N*-glycosidase F (NEB P0705S) in 100 μL of 100 mM ammonium bicarbonate (pH 8) prepared in ^{18}O-labeled water (97 atom % ^{18}O; Sigma). The enzymatic reaction was performed overnight at 37°C. The supernatant containing released glycans was removed, and samples were subjected to in-gel tryptic digestion (Shevchenko et al., 2006). LC-MS/MS analyses were carried out on an Ultimate 3000 Nanoflow HPLC system (Dionex) coupled via a nonospray interface to an LTQ Orbitrap XL mass spectrometer (Thermo Scientific). A concatenated target-decoy database consisting of Arabidopsis representative gene models (The Arabidopsis Information Resource 10; January 3, 2011) supplemented with a list of common contaminants (common Repository of Adventitious Proteins; February 29, 2012; ftp://ftp.thegpm.org/fasta/cRAP/) and the polypeptide sequence of wild-type peptide-*N*-glycosidase F from *Elizabethkingia meningoseptica* (UniProtKB code P21163) was used for peptide identification using X!Tandem (version 2013.09.01; Craig and Beavis, 2004). Decoy sequences were generated by amino acid shuffling of tryptic peptide sequences. For details regarding instrument settings, peptide identification, and data analysis, refer to Mathieu-Rivet et al. (2013).

Determination of Protein and Chlorophyll Content

Measurements of protein concentration were done using the Bio-Rad Protein Assay. Chlorophyll content was determined according to Porra et al. (1989).

Preparation of AtFD1- and AtFD2-Bound Protein Samples

Mature sequences of AtFD1 and AtFD2 proteins were expressed in *Escherichia coli* and purified as described (Hanke et al., 2004), after which the proteins were covalently bound to Sepharose resin (Hanke et al., 2011). Crude protein fractions were prepared from Arabidopsis leaves by grinding at 4°C in 50 mM Tris-HCl, pH 7.5, 100 mM NaCl, and 0.1% (v/v) Triton X-100, with Complete Protease Inhibitor Cocktail, in the presence of preswollen polyvinylpolypyrrolidone. Particulate matter was removed by centrifugation at 4°C and 11,000*g*, and the resulting solution was desalted into 50 mM Tris-HCl,

pH 7.5, over Sephadex G-25 before being used to challenge a column made of the AtFD-bound resin. Following extensive washing, bound proteins were eluted with 50 mM Tris-HCl, pH 7.5, and 500 mM NaCl and concentrated for further analysis with Amicon spin concentrators with a 30-kD cutoff (Millipore).

One-Dimensional SDS-PAGE

Proteins were separated in the linear range for each primary antibody using SDS-PAGE (12%–15% [w/v] acrylamide). The phosphorylation status of AtFNR was studied using Phos-tag acrylamide gels (Wako Pure Chemical Industries), 150 μM Phos-tag ligand, and 2.3 μmol of $MnCl_2$. After gel electrophoresis, the Phos-tag gels were incubated in transfer buffer containing 1 mmol of EDTA prior to western blotting.

2D Electrophoresis

Immobiline DryStrip gels (IPG strips; pH 3–11 NL, 18 cm; GE Healthcare Life Sciences) were rehydrated in rehydration buffer (8 M urea, 2 M thiourea, 4% [w/v] CHAPS, 100 mM dithiothreitol, and 0.5% [v/v] IPG buffer, pH 3–11 NL) overnight. A total of 200 μg of protein (membrane, soluble, or stroma) extract was solubilized with rehydration buffer in a final volume of 150 μL by vortexing for 2 to 3 h at room temperature and loaded into rehydrated IPG strips via cup loading. The first-dimension separation was performed using the Ettan IPGphor 3 isoelectric focusing system. The proteins were focused at 150 V for 3 h and at 300 V for 3 h, then the voltage was raised to 1,000 V during 6 h and to 10,000 V during 2 h, and then kept at 10,000 V for 3 h. After isoelectric focusing, the IPG strips were treated for 15 min with equilibration solution (0.375 M Tris-HCl, pH 8.8, 6 M urea, 30% [w/v] glycerol, and 2% [w/v] SDS) containing 130 mM dithiothreitol and for 15 min with equilibration solution containing 135 mM iodoacetamide. The second dimension separation was carried out by linear SDS-PAGE (14% [w/v] acrylamide), and the gels were silver stained using standard methods.

BN-PAGE

Thylakoid protein complexes were separated using BN-PAGE as described (Lintala et al., 2009).

Immunoblotting and Quantification

After gel electrophoresis, proteins were electroblotted to a polyvinylidene fluoride membrane (Immobilon-P; Millipore). Immunolabeling was carried out using protein-specific primary antibodies. The FNR antibody was a kind gift from Henrik V. Scheller (Andersen et al., 1992). Horseradish peroxidase-conjugated anti-rabbit secondary antibody (GE Healthcare) with ECL Western Blotting Detection Reagents (GE Healthcare) were used for the detection of proteins on x-ray films (Fujifilm SuperRX).

Blots were imaged using the Geliance 1000 imager and GeneSnap imaging software (PerkinElmer). 2D blots were quantified using the ProFINDER 2D Gel Analysis software (PerkinElmer).

MS Analysis and N-Terminal Sequencing

For MS analysis of PTMs, protein spots were excised from silver-stained 2D gels and in-gel digested with trypsin according to Shevchenko et al. (2006). LC-MS/MS analyses were performed on a nanoflow HPLC system (Easy-Nano; Thermo Fisher Scientific) coupled to the LTQ Orbitrap Velos Pro mass spectrometer (Thermo Fisher Scientific). Peptides were first loaded on a trapping column and subsequently separated inline on an in-house-made 15-cm C18 column (75 μm × 15 cm, Magic 5-μm, 200-Å C_{18}; Michrom BioResources). The mobile phase consisted of a mixture of water:acetonitrile (98:2, v/v) with 0.2% (v/v) formic acid (solvent A) and acetonitrile:water (95:5, v/v) with 0.2% (v/v) formic acid (solvent B). A linear 20-min gradient from 5% to 35% (v/v) B was used to elute peptides. Mass spectra were acquired in a data-dependent manner with an automatic switch between MS and tandem MS scans using a top-10 method. Peptide fragmentation was performed with collision-induced dissociation.

The data files were searched for protein identification and modifications using Proteome Discoverer (version 1.4) connected to in-house Mascot (version 2.4) software. To detect Lys acetylation and methylation, data were searched against the SwissProt database (release 2011_08) by using Arabidopsis as a taxonomy filter. To observe the N-terminal peptides, data were searched against an in-house-made database consisting of reviewed canonical Arabidopsis proteins (SwissProt; release 2014_02) and common laboratory contaminants. Database search settings included precursor mass tolerance of 5 ppm, fragment mass tolerance of 0.5 D, semitryptic peptides, one missed trypsin cleavage, fixed modification of carbamidomethylation of Cys, variable modifications of Met oxidation, acetylation of Lys or peptide N terminus, and methylation of Lys or Arg. A significance threshold of $P < 0.05$ was used. To confirm acetylation sites, a manual verification of the matched spectrum was performed.

For N-terminal sequencing, 2D-separated proteins were electroblotted to a polyvinylidene fluoride membrane (Immobilon-P; Millipore) followed by Coomassie Brilliant Blue staining. The AtFNR spots were excised, and N-terminal sequencing was performed using the Procise 494A sequencer (PerkinElmer).

Structural Modeling

For homology modeling of the complex between AtFNR1, AtFNR2, and AtTIC62, a modified version of the crystal structure of PsFNR in complex with PsTIC62 (PDB code 3MHP; Alte et al., 2010) was used as a template. $NADP^+$ was included in the model by superimposing the structure of PsFNR with $NADP^+$ (PDB code 1QFY; Deng et al., 1999) on top of the PsFNR-TIC62 complex structure and saving the $NADP^+$ molecule into this structure. Additionally, rotamers of Tyr-308 in the PsFNR-TIC62 complex structure were checked in the BODIL modeling environment (Lehtonen et al., 2004), and the only rotamer allowing access to the $NADP^+$-binding site was selected. The resulting structure was a PsFNR-TIC62 complex with bound FAD and $NADP^+$, which was then used as a template for modeling the AtFNR1-FNR2 heterodimer in complex with AtTIC62, FAD, and $NADP^+$. The AtFNR1, AtFNR2, and AtTIC62 sequences were downloaded from UniProtKB (accession codes Q9FKW6, Q8W493, and Q8H0U5, respectively) and aligned to PsFNR and PsTIC62 with MALIGN (Johnson et al., 1996) in the BODIL modeling environment (Lehtonen et al., 2004). The sequence identity between PsFNR and AtFNR1 is 89.5%, while the identity for AtFNR2 is 84.8%. The PsTIC62 peptide shares 69.2% identity with the corresponding region in AtTIC62. Based on the template crystal structure, amino acids Ser-66 to Thr-360 from AtFNR1, Ser-75 to Thr-369 from AtFNR2, and Lys-440 to Ser-465 from AtTIC62 could be modeled. A set of 10 models was created with MODELLER (Sali and Blundell, 1993), and the model with the lowest value of the MODELLER objective function was chosen as the best model. Model evaluations were performed with PROCHECK (Laskowski et al., 1993) and QMEAN (Benkert et al., 2009). Alignment images were created with ESPript (version 3.0; Gouet et al., 2003) and model images with PyMOL (version 1.6; Schrödinger).

Sequence data from this article can be found in the Arabidopsis Genome Initiative or UniProtKB databases under the following accession numbers: AtFNR1 (At5g66190/Q9FKW6), AtFNR2 (At1g20020/Q8W493), AtFD1 (At1g10960), AtFD2 (At1g60950), AtTIC62 (At3g18890/ Q8H0U5), AtTROL (At4g01050), and ZmFD (P27787).

Supplemental Data

The following materials are available in the online version of this article.

Supplemental Figure S1. The conserved *N*-glycosylation site in the plant-type FNRs.

Supplemental Figure S2. Phosphorylation of AtFNR isoforms.

Supplemental Figure S3. Glycosylation of AtFNR.

Supplemental Figure S4. Sequence alignment of ZmFNR, PsFNR, AtFNR1, and AtFNR2.

Supplemental Figure S5. Sequence alignment of ZmFD, AtFD1, and AtFD2.

Supplemental Table S1. MS analysis of AtFNR1 and AtFNR2 N-terminal peptides from the chloroplast membrane and stromal fractions.

Supplemental Table S2. Detection of glycosylated peptides in the acidic and basic membrane-bound AtFNR1 and AtFNR2 proteins.

ACKNOWLEDGMENTS

We thank Dr. Andrea Trotta for fruitful discussions, Ilaf Bilal and Markus Palonen for skillful technical assistance, Dr. Taina Tyystjärvi for critical reading of the article, and Mark S. Johnson and Biocenter Finland (bioinformatics, structural biology, and translational activities) for the excellent computational infrastructure at the Structural Bioinformatics Laboratory, Åbo Akademi University.

Received August 26, 2014; accepted October 7, 2014; published October 9, 2014.

LITERATURE CITED

Alban C, Tardif M, Mininno M, Brugière S, Gilgen A, Ma S, Mazzoleni M, Gigarel O, Martin-Laffon J, Ferro M, et al (2014) Uncovering the protein lysine and arginine methylation network in Arabidopsis chloroplasts. PLoS ONE **9:** e95512

Aliverti A, Deng Z, Ravasi D, Piubelli L, Karplus PA, Zanetti G (1998) Probing the function of the invariant glutamyl residue 312 in spinach ferredoxin-NADP$^+$ reductase. J Biol Chem **273:** 34008–34015

Alte F, Stengel A, Benz JP, Petersen E, Soll J, Groll M, Bölter B (2010) Ferredoxin:NADPH oxidoreductase is recruited to thylakoids by binding to a polyproline type II helix in a pH-dependent manner. Proc Natl Acad Sci USA **107:** 19260–19265

Andersen B, Scheller HV, Møller BL (1992) The PSI-E subunit of photosystem I binds ferredoxin:NADP$^+$ oxidoreductase. FEBS Lett **311:** 169–173

Aro E-M, Virgin I, Andersson B (1993) Photoinhibition of photosystem II: inactivation, protein damage and turnover. Biochim Biophys Acta **1143:** 113–134

Benkert P, Künzli M, Schwede T (2009) QMEAN server for protein model quality estimation. Nucleic Acids Res **37:** W510–W514

Benz JP, Lintala M, Soll J, Mulo P, Bölter B (2010) A new concept for ferredoxin-NADP(H) oxidoreductase binding to plant thylakoids. Trends Plant Sci **15:** 608–613

Benz JP, Stengel A, Lintala M, Lee YH, Weber A, Philippar K, Gügel IL, Kaieda S, Ikegami T, Mulo P, et al (2009) *Arabidopsis* Tic62 and ferredoxin-NADP(H) oxidoreductase form light-regulated complexes that are integrated into the chloroplast redox poise. Plant Cell **21:** 3965–3983

Bienvenut WV, Espagne C, Martinez A, Majeran W, Valot B, Zivy M, Vallon O, Adam Z, Meinnel T, Giglione C (2011) Dynamics of post-translational modifications and protein stability in the stroma of *Chlamydomonas reinhardtii* chloroplasts. Proteomics **11:** 1734–1750

Bienvenut WV, Sumpton D, Martinez A, Lilla S, Espagne C, Meinnel T, Giglione C (2012) Comparative large scale characterization of plant versus mammal proteins reveals similar and idiosyncratic N-α-acetylation features. Mol Cell Proteomics **11:** 015131

Bischof S, Baerenfaller K, Wildhaber T, Troesch R, Vidi PA, Roschitzki B, Hirsch-Hoffmann M, Hennig L, Kessler F, Gruissem W, et al (2011) Plastid proteome assembly without Toc159: photosynthetic protein import and accumulation of *N*-acetylated plastid precursor proteins. Plant Cell **23:** 3911–3928

Bowsher CG, Eyres LM, Gummadova JO, Hothi P, McLean KJ, Munro AW, Scrutton NS, Hanke GT, Sakakibara Y, Hase T (2011) Identification of N-terminal regions of wheat leaf ferredoxin NADP$^+$ oxidoreductase important for interactions with ferredoxin. Biochemistry **50:** 1778–1787

Choudhary C, Kumar C, Gnad F, Nielsen ML, Rehman M, Walther TC, Olsen JV, Mann M (2009) Lysine acetylation targets protein complexes and co-regulates major cellular functions. Science **325:** 834–840

Craig R, Beavis RC (2004) TANDEM: matching proteins with tandem mass spectra. Bioinformatics **20:** 1466–1467

Deng Z, Aliverti A, Zanetti G, Arakaki AK, Ottado J, Orellano EG, Calcaterra NB, Ceccarelli EA, Carrillo N, Karplus PA (1999) A productive NADP$^+$ binding mode of ferredoxin-NADP$^+$ reductase revealed by protein engineering and crystallographic studies. Nat Struct Biol **6:** 847–853

Ferro M, Salvi D, Brugière S, Miras S, Kowalski S, Louwagie M, Garin J, Joyard J, Rolland N (2003) Proteomics of the chloroplast envelope membranes from *Arabidopsis thaliana*. Mol Cell Proteomics **2:** 325–345

Finkemeier I, Laxa M, Miguet L, Howden AJ, Sweetlove LJ (2011) Proteins of diverse function and subcellular location are lysine acetylated in Arabidopsis. Plant Physiol **155:** 1779–1790

Gouet P, Robert X, Courcelle E (2003) ESPript/ENDscript: extracting and rendering sequence and 3D information from atomic structures of proteins. Nucleic Acids Res **31:** 3320–3323

Gummadova JO, Fletcher GJ, Moolna A, Hanke GT, Hase T, Bowsher CG (2007) Expression of multiple forms of ferredoxin NADP$^+$ oxidoreductase in wheat leaves. J Exp Bot **58:** 3971–3985

Hanke G, Mulo P (2013) Plant type ferredoxins and ferredoxin-dependent metabolism. Plant Cell Environ **36:** 1071–1084

Hanke GT, Endo T, Satoh F, Hase T (2008) Altered photosynthetic electron channelling into cyclic electron flow and nitrite assimilation in a mutant of ferredoxin:NADP(H) reductase. Plant Cell Environ **31:** 1017–1028

Hanke GT, Kimata-Ariga Y, Taniguchi I, Hase T (2004) A post genomic characterization of Arabidopsis ferredoxins. Plant Physiol **134:** 255–264

Hanke GT, Okutani S, Satomi Y, Takao T, Suzuki A, Hase T (2005) Multiple iso-proteins of FNR in Arabidopsis: evidence for different contributions to chloroplast function and nitrogen assimilation. Plant Cell Environ **28:** 1146–1157

Hanke GT, Satomi Y, Shinmura K, Takao T, Hase T (2011) A screen for potential ferredoxin electron transfer partners uncovers new, redox dependent interactions. Biochim Biophys Acta **1814:** 366–374

Hirohashi T, Hase T, Nakai M (2001) Maize non-photosynthetic ferredoxin precursor is missorted to the intermembrane space of chloroplasts in the presence of light. Plant Physiol **125:** 2154–2163

Hodges M, Miginiac-Maslow M, Le Maréchal P, Rémy R (1990) The ATP-dependent post translational modification of ferredoxin:NADP$^+$ oxidoreductase. Biochim Biophys Acta **1052:** 446–452

Hoshiyasu S, Kohzuma K, Yoshida K, Fujiwara M, Fukao Y, Yokota A, Akashi K (2013) Potential involvement of N-terminal acetylation in the quantitative regulation of the ε subunit of chloroplast ATP synthase under drought stress. Biosci Biotechnol Biochem **77:** 998–1007

Houtz RL, Poneleit L, Jones SB, Royer M, Stults JT (1992) Posttranslational modifications in the amino-terminal region of the large subunit of ribulose-1,5-bisphosphate carboxylase/oxygenase from several plant species. Plant Physiol **98:** 1170–1174

Hurley JK, Salamon Z, Meyer TE, Fitch JC, Cusanovich MA, Markley JL, Cheng H, Xia B, Chae YK, Medina M, et al (1993) Amino acid residues in *Anabaena* ferredoxin crucial to interaction with ferredoxin-NADP$^+$ reductase: site-directed mutagenesis and laser flash photolysis. Biochemistry **32:** 9346–9354

Jelesarov I, Bosshard HR (1994) Thermodynamics of ferredoxin binding to ferredoxin:NADP$^+$ reductase and the role of water at the complex interface. Biochemistry **33:** 13321–13328

Jenuwein T, Allis CD (2001) Translating the histone code. Science **293:** 1074–1080

Johnson MS, May AC, Rodionov MA, Overington JP (1996) Discrimination of common protein folds: application of protein structure to sequence/structure comparisons. Methods Enzymol **266:** 575–598

Jurić S, Hazler-Pilepić K, Tomasić A, Lepedus H, Jelicić B, Puthiyaveetil S, Bionda T, Vojta L, Allen JF, Schleiff E, et al (2009) Tethering of ferredoxin: NADP$^+$ oxidoreductase to thylakoid membranes is mediated by novel chloroplast protein TROL. Plant J **60:** 783–794

Kleffmann T, von Zychlinski A, Russenberger D, Hirsch-Hoffmann M, Gehrig P, Gruissem W, Baginsky S (2007) Proteome dynamics during plastid differentiation in rice. Plant Physiol **143:** 912–923

Kurisu G, Kusunoki M, Katoh E, Yamazaki T, Teshima K, Onda Y, Kimata-Ariga Y, Hase T (2001) Structure of the electron transfer complex between ferredoxin and ferredoxin-NADP$^+$ reductase. Nat Struct Biol **8:** 117–121

Laskowski RA, Moss DS, Thornton JM (1993) Main-chain bond lengths and bond angles in protein structures. J Mol Biol **231:** 1049–1067

Lee YH, Ikegami T, Standley DM, Sakurai K, Hase T, Goto Y (2011) Binding energetics of ferredoxin-NADP$^+$ reductase with ferredoxin and its relation to function. ChemBioChem **12:** 2062–2070

Lehtonen JV, Still DJ, Rantanen VV, Ekholm J, Björklund D, Iftikhar Z, Huhtala M, Repo S, Jussila A, Jaakkola J, et al (2004) BODIL: a molecular modeling environment for structure-function analysis and drug design. J Comput Aided Mol Des **18:** 401–419

Lintala M, Allahverdiyeva Y, Kangasjärvi S, Lehtimäki N, Keränen M, Rintamäki E, Aro EM, Mulo P (2009) Comparative analysis of leaf-type ferredoxin-NADP oxidoreductase isoforms in *Arabidopsis thaliana*. Plant J **57:** 1103–1115

Lintala M, Allahverdiyeva Y, Kidron H, Piippo M, Battchikova N, Suorsa M, Rintamäki E, Salminen TA, Aro EM, Mulo P (2007) Structural and

functional characterization of ferredoxin-NADP$^+$-oxidoreductase using knock-out mutants of Arabidopsis. Plant J **49:** 1041–1052

Lintala M, Lehtimäki N, Benz JP, Jungfer A, Soll J, Aro EM, Bölter B, Mulo P (2012) Depletion of leaf-type ferredoxin-NADP$^+$ oxidoreductase results in the permanent induction of photoprotective mechanisms in Arabidopsis chloroplasts. Plant J **70:** 809–817

Lintala M, Schuck N, Thormählen I, Jungfer A, Weber KL, Weber AP, Geigenberger P, Soll J, Bölter B, Mulo P (2014) Arabidopsis *tic62 trol* mutant lacking thylakoid-bound ferredoxin-NADP$^+$ oxidoreductase shows distinct metabolic phenotype. Mol Plant **7:** 45–57

Mann M, Jensen ON (2003) Proteomic analysis of post-translational modifications. Nat Biotechnol **21:** 255–261

Martínez-Júlvez M, Medina M, Velázquez-Campoy A (2009) Binding thermodynamics of ferredoxin:NADP$^+$ reductase: two different protein substrates and one energetics. Biophys J **96:** 4966–4975

Mathieu-Rivet E, Scholz M, Arias C, Dardelle F, Schulze S, Le Mauff F, Teo G, Hochmal AK, Blanco-Rivero A, Loutelier-Bourhis C, et al (2013) Exploring the N-glycosylation pathway in *Chlamydomonas reinhardtii* unravels novel complex structures. Mol Cell Proteomics **12:** 3160–3183

Meinnel T, Peynot P, Giglione C (2005) Processed N-termini of mature proteins in higher eukaryotes and their major contribution to dynamic proteomics. Biochimie **87:** 701–712

Michel H, Hunt DF, Shabanowitz J, Bennett J (1988) Tandem mass spectrometry reveals that three photosystem II proteins of spinach chloroplasts contain N-acetyl-O-phosphothreonine at their NH_2 termini. J Biol Chem **263:** 1123–1130

Mininno M, Brugière S, Pautre V, Gilgen A, Ma S, Ferro M, Tardif M, Alban C, Ravanel S (2012) Characterization of chloroplastic fructose 1,6-bisphosphate aldolases as lysine-methylated proteins in plants. J Biol Chem **287:** 21034–21044

Moolna A, Bowsher CG (2010) The physiological importance of photosynthetic ferredoxin NADP$^+$ oxidoreductase (FNR) isoforms in wheat. J Exp Bot **61:** 2669–2681

Morales R, Kachalova G, Vellieux F, Charon MH, Frey M (2000) Crystallographic studies of the interaction between the ferredoxin-NADP$^+$ reductase and ferredoxin from the cyanobacterium *Anabaena*: looking for the elusive ferredoxin molecule. Acta Crystallogr D Biol Crystallogr **56:** 1408–1412

Mulligan RM, Houtz RL, Tolbert NE (1988) Reaction-intermediate analogue binding by ribulose bisphosphate carboxylase/oxygenase causes specific changes in proteolytic sensitivity: the amino-terminal residue of the large subunit is acetylated proline. Proc Natl Acad Sci USA **85:** 1513–1517

Nanjo Y, Oka H, Ikarashi N, Kaneko K, Kitajima A, Mitsui T, Muñoz FJ, Rodríguez-López M, Baroja-Fernández E, Pozueta-Romero J (2006) Rice plastidial N-glycosylated nucleotide pyrophosphatase/phosphodiesterase is transported from the ER-Golgi to the chloroplast through the secretory pathway. Plant Cell **18:** 2582–2592

Pesaresi P, Gardner NA, Masiero S, Dietzmann A, Eichacker L, Wickner R, Salamini F, Leister D (2003) Cytoplasmic N-terminal protein acetylation is required for efficient photosynthesis in *Arabidopsis*. Plant Cell **15:** 1817–1832

Plöscher M, Granvogl B, Reisinger V, Eichacker LA (2009) Identification of the N-termini of NADPH:protochlorophyllide oxidoreductase A and B from barley etioplasts (*Hordeum vulgare* L.). FEBS J **276:** 1074–1081

Porra RJ, Thompson WA, Kriedemann PE (1989) Determination of accurate extinction coefficients and simultaneous equations for assaying chlorophylls *a* and *b* extracted with four different solvents: verification of the concentration of chlorophyll standards by atomic absorption spectroscopy. Biochim Biophys Acta **975:** 384–394

Prabakaran S, Lippens G, Steen H, Gunawardena J (2012) Post-translational modification: nature's escape from genetic imprisonment and the basis for dynamic information encoding. Wiley Interdiscip Rev Syst Biol Med **4:** 565–583

Reiland S, Messerli G, Baerenfaller K, Gerrits B, Endler A, Grossmann J, Gruissem W, Baginsky S (2009) Large-scale Arabidopsis phosphoproteome profiling reveals novel chloroplast kinase substrates and phosphorylation networks. Plant Physiol **150:** 889–903

Sali A, Blundell TL (1993) Comparative protein modelling by satisfaction of spatial restraints. J Mol Biol **234:** 779–815

Shevchenko A, Tomas H, Havlis J, Olsen JV, Mann M (2006) In-gel digestion for mass spectrometric characterization of proteins and proteomes. Nat Protoc **1:** 2856–2860

Strasser R, Stadlmann J, Svoboda B, Altmann F, Glössl J, Mach L (2005) Molecular basis of N-acetylglucosaminyltransferase I deficiency in *Arabidopsis thaliana* plants lacking complex N-glycans. Biochem J **387:** 385–391

Sugiyama N, Nakagami H, Mochida K, Daudi A, Tomita M, Shirasu K, Ishihama Y (2008) Large-scale phosphorylation mapping reveals the extent of tyrosine phosphorylation in Arabidopsis. Mol Syst Biol **4:** 193

Tikkanen M, Aro EM (2012) Thylakoid protein phosphorylation in dynamic regulation of photosystem II in higher plants. Biochim Biophys Acta **1817:** 232–238

Twachtmann M, Altmann B, Muraki N, Voss I, Okutani S, Kurisu G, Hase T, Hanke GT (2012) N-terminal structure of maize ferredoxin: NADP$^+$ reductase determines recruitment into different thylakoid membrane complexes. Plant Cell **24:** 2979–2991

Villarejo A, Burén S, Larsson S, Déjardin A, Monné M, Rudhe C, Karlsson J, Jansson S, Lerouge P, Rolland N, et al (2005) Evidence for a protein transported through the secretory pathway en route to the higher plant chloroplast. Nat Cell Biol **7:** 1224–1231

Walling LL (2006) Recycling or regulation? The role of amino-terminal modifying enzymes. Curr Opin Plant Biol **9:** 227–233

Wu X, Oh MH, Schwarz EM, Larue CT, Sivaguru M, Imai BS, Yau PM, Ort DR, Huber SC (2011) Lysine acetylation is a widespread protein modification for diverse proteins in Arabidopsis. Plant Physiol **155:** 1769–1778

Xing S, Poirier Y (2012) The protein acetylome and the regulation of metabolism. Trends Plant Sci **17:** 423–430

Yang Z, Guo G, Zhang M, Liu CY, Hu Q, Lam H, Cheng H, Xue Y, Li J, Li N (2013) Stable isotope metabolic labeling-based quantitative phosphoproteomic analysis of Arabidopsis mutants reveals ethylene-regulated time-dependent phosphoproteins and putative substrates of constitutive triple response 1 kinase. Mol Cell Proteomics **12:** 3559–3582

Zhang L, Paakkarinen V, van Wijk KJ, Aro EM (1999) Co-translational assembly of the D1 protein into photosystem II. J Biol Chem **274:** 16062–16067

Zybailov B, Rutschow H, Friso G, Rudella A, Emanuelsson O, Sun Q, van Wijk KJ (2008) Sorting signals, N-terminal modifications and abundance of the chloroplast proteome. PLoS ONE **3:** e1994